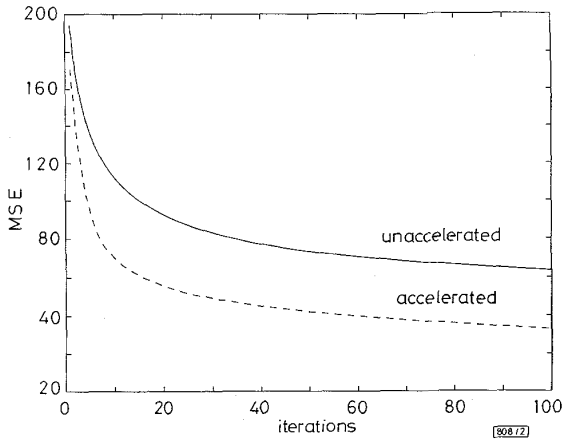

Fig. 2 *Mean-square error between restoration and original unblurred image (no noise)*

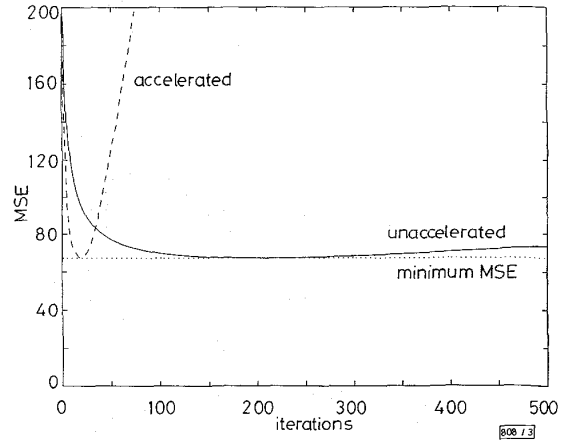

Fig. 3 *Mean-square error between restoration and original unblurred image (unit variance noise)*

The acceleration algorithm was also tested in the presence of noise. The image was corrupted by additive Gaussian noise with unit variance. Fig. 3 shows the MSE between the original and restored image. The MSE drops initially, but then increases as the R-L restoration attempts to overfit the noisy data causing a less desirable result. The minimum MSE is indicated by the dotted line and occurs after 201 unaccelerated iterations or 19 accelerated iterations, a speedup of 10.6 times.

An analysis of the MSE curves for several different images and PSFs, shows if an unaccelerated restoration requires N iterations then the equivalent accelerated restoration requires $O(\sqrt{N})$ iterations. In the example presented a restoration with N_U unaccelerated iterations is equivalent to N_A accelerated iterations with

$$N_A \simeq 1.5\sqrt{N_U} - 1 \qquad (10)$$

Conclusion: The acceleration of the convergence of the iterative R-L restoration algorithm has been investigated. A conjugate gradient technique with an MMSE criterion has been used to accelerate the convergence of the R-L image restoration algorithm. The acceleration method is simple to calculate and produces significantly higher levels of acceleration than previous methods.

5 September 1995
Electronics Letters Online No: 19951400

D.S.C. Biggs and M. Andrews (*Department of Electrical and Electronic Engineering, University of Auckland, Private Bag 92019, New Zealand*)

References

1 RICHARDSON, W.H.: 'Bayesian-based iterative method of image restoration', *J. Opt. Soc. Am.*, 1972, **62**, (1), pp. 55–59
2 LUCY, L.B.: 'An iterative technique for the rectification of observed images', *Astron.J.*, 1974, **79**, (6), pp. 745–754
3 KAUFMAN, L.: 'Implementing and accelerating the EM algorithm for positron emission tomography', *IEEE Trans. Med. Imaging*, 1987, **6**, (1), pp. 37–51
4 HOLMES, T.J., and LIU, Y.-H.: 'Acceleration of maximum-likelihood image restoration for fluorescence microscopy and other noncoherent imagery', *J. Opt. Soc. Am. A*, 1991, **8**, (6), pp. 893–907
5 ADORF, H.M., HOOK, R.N., LUCY, L.B., and MURTAGH, F.D.: 'Accelerating the Richardson-Lucy restoration algorithm'. Proc. 4th ESO/ST-ECF Data Analysis Workshop, European Southern Observatory, 1992, pp. 99–103
6 PRESS, W.H., TEUKILSKY, S.A., VETTERLING, W.T., and FLANNERY, B.P.: 'Numerical recipes in C: The art of scientific computing' (Cambridge University Press, 1992), 2nd Edn.

Genetic-based fuzzy hit-or-miss texture spectrum for texture analysis

Yih-Gong Lee, Jia-Hong Lee and Yuang-Cheh Hsueh

Indexing terms: Genetic algorithms, Texture (image processing)

A new method using a fuzzy hit-or-miss transform recognition procedure, which measures degrees of fit of specified patterns within an image, is proposed for texture analysis. For a given texture, three optimal texture patterns (structuring elements) dynamically generated by genetic algorithms are used to inspect the degrees of fit by using the fuzzy hit-or-miss transform, respectively. The distribution of these degrees of fit, converted into a texture spectrum, is used as the texture feature for texture analysis.

Introduction: Texture analysis is one of the important techniques in image processing. The major problem of texture analysis is the extraction of texture features. The general methods for feature extraction are to estimate local features at each pixel in a texture image, and then derive a set of statistics from the distributions of the local features. The surveys and comparisons of different methods for feature extraction can be found in [1, 2].

A new method for texture feature extraction based on fuzzy theory is presented. Fuzzy set theory [3] is a mathematical tool in modelling ambiguity or uncertainty and has been applied to texture analysis [4]. In texture analysis, we define the 'fuzzy hit-or-miss transform', which ranges from 0 to 1, for a block B in the texture as the degree of fit to a given specified structuring element (SE). Therefore, we can transform a grey-scale image into a fuzzy image by using the transform. The fuzzy image membership distribution, denoted as the fuzzy hit-or-miss texture spectrum (FHMTS), is then used as a distinguishing feature for texture analysis. For texture classification, the selection of the SE is important since the size and content of the employed SE for input texture determines the accuracy of texture classification. To gain a superior accuracy rate of texture classification, we use genetic algorithms (GAs) to dynamically generate three optimal SEs according to the characteristics of input texture.

Fuzzy hit-or-miss texture spectrum: The fuzzy hit-or-miss transform [5] is difficult to apply in grey-scale images. Therefore, thresholding for grey level texture images into binary images is necessary in our application and the following procedure is used: if $I(x, y) \geq \mu$ then $f(x, y) = 1$ otherwise $f(x, y) = 0$, where I is a grey level image, μ is the mean value of I, and f is the output binary image. Let $g^*(x, y) = 1 - g(x, y)$ be the dual template of g; the fuzzy hit-or-miss transform is defined as

$$[f \circledast (g, g^*)](x, y) = \psi[\alpha(x, y), \beta(x, y)] \qquad (1)$$

where ψ is a real-valued function (here, average operator is used) such that $\psi[\alpha(x, y), \beta(x, y)] \in [0,1]$, and $\alpha(x, y) = [\Sigma_{D_g} f \ominus g]/A(g)$, $\beta(x, y) = [\Sigma_{D_g^*} f^c \ominus g^*]/A(g^*)$ where the operator $\ominus$ is the morphological erosion [6] and f^c is the complement of binary image f. $A(g)$ and $A(g^*)$ are the area (number of pixels) of the template g and g^*, D_g and D_g^* are the domains of g and g^*.

The fuzzy hit-or-miss transform can be considered as a pattern matched degree filter. It allows both for partial and exact occurrence of the dual templates g, g^*. Therefore, we use the fuzzy hit-or-miss transform to analyse textures in our experiments. In a fuzzy image, the member with fit value 0 represents the corresponding subimage being the complement of the *SE*, 1 represents the corresponding subimage being the same with the *SE*. The greater the fit value, the more a given pattern is revealed.

To analyse a texture image, we transform it into its corresponding fuzzy image using eqn. 1. As the value in the fuzzy image represents the local aspect, the statistics of these values in the fuzzy image should reveal its texture information. The occurrence distribution of these values is the FHMTS, with the abscissa indicating the degree of fit and the ordinate representing its frequency occurrence . To evaluate the performance of the extracted feature by using the proposed method, we calculated and compared the FHMTS for two Brodatz textures D54 and D77 [7]. The two textures are shown in Fig. 3(*f*) and (*g*) and their corresponding FHMTS using a 5 × 5 square SE are displayed in Fig. 1. From Fig. 1, we find that the measured FHMTSs are distinguishable from each other so they can serve as a good discriminating tool in texture classification. The FHMTS of D54 shows a higher frequency than D77 when the measured degree of fit is close to unity, so that the texture image D54 contains more 5 × 5 square patterns than D77.

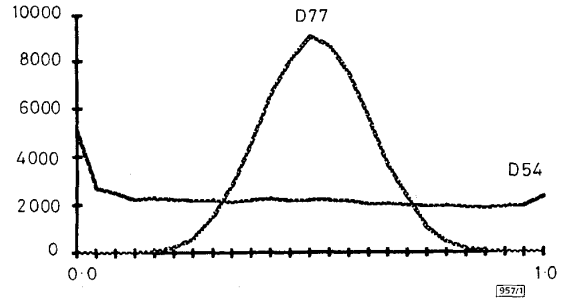

Fig. 1 *FHMTS of textures of D54 and D77*

Genetic-based structuring elements and texture classification: To obtain a superior accuracy rate in texture classification, three optimal *SE*s, which are dynamically generated by GAs [8] according to the input testing texture, are used to compute the FHMTS. To demonstrate the discrimination performance of the GA-based FHMTS, we use a supervised classification with minimum distance rule to classic nature images, extracted from the Brodatz album. Eight 256 × 256 natural images with 256 grey-levels are used for the texture classification (see Fig. 3). Each texture image is divided into 16 nonoverlapping 64 × 64 subimages.

In the training phase, we randomly select a 64 × 64 block from each texture image for GAs training cycle to generate three optimal *SE*s and prototype texture spectra. The representation scheme is to encode a 5 × 5 square into a gene string raw by raw sequentially and a 25-length gene string is obtained. Three different fitness functions and a two-point crossover method are employed since three optimal *SE*s are used in our experiments. The three fitness functions are defined as follows:

$$fit_1(g_m) = \inf D\left(S_{g_m}^{f_i}, S_{g_m}^{f_j}\right) \quad \text{for } i,j = 1,2,\ldots,K \text{ and } i > j \quad (2)$$

$$fit_2(g_m) = \frac{2}{K(K-1)} \sum D\left(S_{g_m}^{f_i}, S_{g_m}^{f_j}\right) \quad \text{for } i,j = 1,2,\ldots,K \text{ and } i > j \quad (3)$$

$$fit_3(g_m) = \sup D\left(S_{g_m}^{f_i}, S_{g_m}^{f_j}\right) \quad \text{for } i,j = 1,2,\ldots,K \text{ and } i > j \quad (4)$$

where $S^{f_i}_{g_m}$ is the spectrum of texture f_i by using structuring element g_m, where $m = 24$ is the size of the population, K is the number of texture type and $D(S^{f_i}_{g_m}, S^{f_j}_{g_m})$ is the Hamming distance between $S^{f_i}_{g_m}$ and $S^{f_j}_{g_m}$. The Hamming distance is defined as

$$D\left(S_{g_m}^{f_i}, S_{g_m}^{f_j}\right) = \sum_{k=0}^{L-1} \left|S_{g_m}^{f_i}(k) - S_{g_m}^{f_j}(k)\right| \quad (5)$$

where L is the uniformly quantised levels of the degree of fit values (range from 0 to 1) in a fuzzy image and 25 levels are used in our experiments to reduce the calculation time for the pursuit statistics. By iterative running of the evolution cycle, gene strings are updated and the performance is gradually improved. The cycle terminates when all gene strings no longer change, i.e. the gene strings converge. The constructed three optimal *SE*s according to the input eight texture images are displayed in Fig. 2.

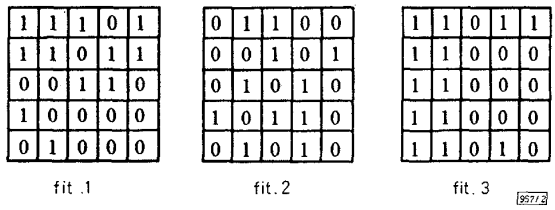

Fig. 2 *Three optimal SEs obtained from different fitness functions*

In the classification phase, we calculate the texture spectra for each considered test subimage by the three optimal *SE*s and compute their summation distance to the prototype texture spectra of each texture type using eqn. 5. The test subimage will be assigned to one of the texture types by using the minimum distance rule and this experimental result shows 96.9% average accuracy rate.

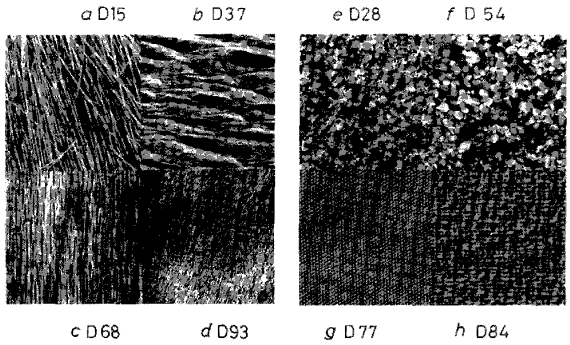

Fig. 3 *Eight texture images extracted from Brodatz album*

Conclusion: A new method using GAs and FHMTS has been proposed for texture analysis. In this method, the local texture feature for a given block is characterised by its corresponding degree of fit , and the global texture aspect of an image is revealed by its texture spectrum. Promising results have been obtained with an accuracy classification rate of 96.9% by using three optimal basic *SE*s. From the experimental results, we conclude that the GA-based FHMTS is an excellent discriminating tool in texture analysis and classification.

Acknowledgments: This work was supported partially by the National Science Council, Republic of China, under grant NSC 84-2213-E-009-045.

25 September 1995
Electronics Letters Online No: 19951398

Yih-Gong Lee, Jia-Hong Lee and Yuang-Cheh Hsueh (*Department of Computer and Information Science, National Chiao Tung University, Hsinchu, Taiwan 30050, Republic of China*)

References

1 REED, T.R., and DU BUF, J.M.H.: 'A review of recent textures segmentation and feature extraction techniques', *CVGIP, Image Underst.*, 1993, **57**, pp. 359–372

2 CONNERS, R.W., and HARLOW, C.A.: 'A theoretical comparison of texture algorithms', *IEEE Trans.*, 1980, **PAMI(2)**, pp. 204–222

3 ZADEH, L.A.: 'Outline of a new approach to the analysis of complex systems and decision processes', *IEEE Trans.*, 1973, **SMC-3**, pp. 28–44

4 LEE, Y.G., LEE, J.A., and HSUEH, Y.C.: 'Fuzzy uncertainty texture spectrum for texture analysis', *Electron. Lett.*, 1995, **31**, (12), pp. 959–960

5 MARAGOS, P.: 'Optimal morphological approaches to image matching and object detection', *Proc. IEEE*, 1988, pp. 695–699

6 SERRA, J.: 'Image analysis and mathematical morphology' (Academic Press, New Yotk, 1982)
7 BRODATZ, P.: 'Textures: A photographic album for artists and designers' (Reinhold Publication, New York, 1968)
8 HOLLAND, J.H.: 'Adaptation in natural and artificial systems: An introductory analysis with applications to biology, control, and artification intelligence' (University of Michigan Press, Ann Arbor, 1975)

Improved discrete cosine transform picture coding by utilising extended Hamming codes

S. Emami and S.L. Miller

Indexing terms: Discrete cosine transforms, Hamming codes, Image coding

In the Letter extended Hamming codes are utilised for error protection of DCT coded pictures. The SNR graphs and the subjective examination of the images demonstrate the effectiveness of the technique.

Introduction: The quality of received DCT coded pictures drops when the channel becomes noisy. A number of approaches to the enhancement of the transform coding method have appeared in the literature [1, 2]. In this Letter, to combat the channel errors, the extended Hamming codes are utilised.

New approach: Consider an (n,k) Hamming code and its extended version $(n+1,k)$. Let d'_{min} and d_{min} denote the minimum distances of the codes, respectively. It is known that $d_{min} = d'_{min}+1$ [3]. The extended Hamming code is superior in terms of error detection capability, it can correct all patterns of $[(d_{min}-1)/2]$ errors and simultaneously detect all patterns of $d_{min}/2$ errors. In our approach, once an error is detected, the value of the coded coefficients is replaced with the average of the same coefficient in the horizontal and vertical directions. This is possible because the low-order DCT coefficients (such as $X(0,0)$, $X(0,1)$, $X(1,0)$ and $X(1,1)$, where $X(k_1,k_2)$ is the DCT of image $x(n_1, n_2)$) vary slightly on a block to block basis.

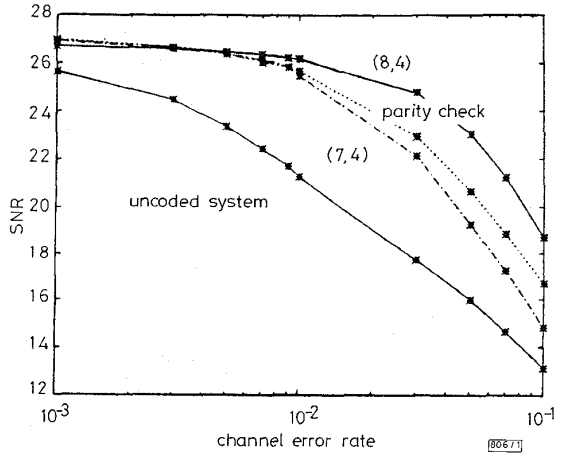

Fig. 1 *Variation of received image SNR against channel error rate for uncoded and coded systems (block size 4×4)*

Results: In the simulations, images were compressed at the rate of 1 bit/pixel. Fig. 1 demonstrates that the use of an (8,4) extended Hamming code is superior to the use of parity or a (7,4) Hamming code when the error rate is >0.01. At an error rate of 0.03, the system employing (8,4) is >7dB superior to the uncoded system.

Conclusions: The use of extended Hamming codes for error protection of DCT coded images results in a larger picture SNR compared to the use of Hamming codes.

5 September 1995
Electronics Letters Online No: 19951383

S. Emami and S.L. Miller (*Department of Electrical Engineering, University of Florida, Gainesville, FL 32611, USA*)

References

1 WONG, W.C., and STEEL, R.: 'Partial correction of transmission errors in Walsh transform image without recourse to error correction coding', *Electron. Lett.*, 1978, **14**, pp. 298–300
2 COMSTOCK, D., and GIBSON, J.D.: 'Hamming coding of DCT compressed images over noisy channels', *IEEE Trans.*, 1984, **COM-32**, pp. 856–861
3 RHEE, M.Y.: 'Error correction coding theory' (McGraw-Hill, 1989)

Quadtree based colour quantisation image compression

L.M. Po, W.T. Tan and W.B. Wong

Indexing terms: Image processing, Data compression, Quadtrees

A new colour quantisation and quadtree based image compression scheme is proposed. The features of the new scheme are that colour palette ordering and requantisation of the decoded image for palette-based monitor displays are not required. Thus, fast decoding and displaying can be achieved.

Introduction: Presently, most low-cost personal computers use 8 bit palette-based graphics architecture for displaying colour images. This means that only 256 colours can be simultaneously displayed. However, conventional colour image compression techniques (such as JPEG) are encoded independently on luminance-chrominance colour spaces. Hence, colour quantisation (CQ) is needed to requantise the decompressed image for palette-based monitor displays. The CQ is a time-consuming operation. To avoid this requantisation operation before displaying the decoded image, it was recently proposed in [1 – 3] to encode and decode the colour image on a palettised image, which represents the colour space defined by an ordered colour palette. Lossy DCT transform coding and sub-band coding were used to encode the palettised image in [1, 2] and [3], respectively. The palettised image was created by ordering the palette and rearranging the index image to suit the lossy compression. In [1, 2], the palette ordering is based on the luminance component whereas a colour correlation method is used in [3]. Even though different schemes were proposed in [1 – 3] to correct the palettised image after decoding, significant visual artifacts owing to lossy encoding of the palettised image may still occurin the reconstructed images. Recently, in our previous work [4], lossless DPCM compression was used to encode the palettised image; this enables visual artifacts owing to lossy encoding of the colour indices in the reconstructed image to be avoided. The redundancy of the palettised image is exploited by the closest pairs colour palette ordering method. However, the performance of these compression techniques [1 – 4] is highly dependent on the ordering of the colour palette. In this Letter, a new quadtree based colour quantisation image compression technique without colour palette ordering is proposed.

Quadtree encoding of colour image: The modified quadtree segmentation encoding algorithm (MQSEA) developed in [5] is adopted in the proposed compression technique. The MQSEA uses a bottom-up quadtree construction procedure, in which recursively small blocks are merged together to form a larger block if they are homogeneous with respect to a merging criterion. The merging criterion for the segmentation of a colour image can be based on distortion measures among the colours of the block. Since a colour pixel can be considered as a 3-D vector $\mathbf{C}_i = [R_i, G_i, B_i]^T$ with components of red, green and blue, the vector distances in RGB space representation of the colour of the block with its neighbouring block's colours can be used as merging criterion of blocks. Unfortunately, RGB space is not a perceptually useful